Microcomputers in Civil Engineering 7 (1992) 91–108

An Approach to Numerical Modelling of Flexible Orbiting Space Structures

V. J. Modi, A. C. Ng & A. Suleman

Department of Mechanical Engineering, The University of British Columbia, Vancouver, British Columbia, Canada V6T 1Z4

Abstract: *A relatively general formulation for studying the dynamics of a large class of spacecraft characterized by interconnected flexible members forming a tree topology is presented. Extremely lengthy, highly nonlinear, nonautonomous, and coupled equations of motion are amenable only to numerical solution using a high performance computer. Discretization of the continuum system is accomplished through either component or system modes obtained through a finite element analysis. Its application is illustrated through two configurations of the evolving Space Station* Freedom. *The modal spectra suggest that: (i) the appendage flexibility plays an important role in governing the system dynamics; (ii) close spacing of the frequencies with possible overlap will make the response extremely complex and the control equally challenging; (iii) the system modes are significantly influenced by the growth of the main truss and module clusters. Versatility of the general formulation is demonstrated through dynamics and control studies of two spacecraft systems: the permanently manned configuration (PMC) of the Space Station; and a system similar to the space flyer unit (SFU) under development in Japan. The PMC study shows that even a small main truss disturbance can excite not only large amplitude motion of the appendages, but also truss velocity and acceleration levels exceeding the specified limit. The deployment of the solar array pedal (SAP) of the SFU shows that the spacecraft remains stable under both symmetric and asymmetric deployments. Advantage of the out-of-plane deployment is also illustrated. The retrieval of the SAP is found to be a difficult task. Only the out-of-plane symmetric retrieval is found to be stable; the in-plane retrieval induces unsatisfactory librational motion. For an asymmetric retrieval, the spacecraft response is unstable and an active control would be required.*

1 INTRODUCTION

With the beginning of the space age in 1957, advent of the Space Shuttle as a platform for structural dynamics experiments in the eighties, and the US commitment to the Space Station *Freedom* by late 1990s, dynamics and control of flexible orbiting structures have become a subject of considerable investigation. A vast body of literature already exists which has been reviewed by Likins & Bouvier,[9] Modi and Shrivastava,[17,20] Roberson,[25] Lips,[10] Ibrahim,[7] Misra and Modi,[14,15] and others.[11,16,30,32] The passage of time clearly suggests a trend towards larger and hence necessarily flexible spacecraft. The progressive increase in dimensions of space vehicles has been governed by several factors:

(i) Ever increasing demand on power for operation of the on board instrumentation, scientific experiments, communication systems, etc., has been reflected in the size of the solar panels. The Canada/USA Communications Technology Satellite (CTS, Hermes) launched in January 1976 carried two solar panels, 1·14 m × 7·32 m each, to generate around 1·2 kW of power. The European Space Agency recently launched the L-SAT (Olympus), which carried solar panels extending to 25 m (tip-to-tip) and advanced models with 33 m panels are to follow.

(ii) Use of large members may be essential in some missions. For example, the Radio Astronomy Explorer (RAE) satellite used four 228·8 m antennae to detect extraterrestrial low frequency signals.

(iii) The Space Shuttle being versatile in undertaking diverse missions, several proposals for its utilization as a platform for conducting structural

Microcomputers in Civil Engineering 0885-9507/92/$05.00

dynamics experiments have been presented. They range over stability and control of large flexible members, manufacturing of structural components for assembly of the proposed Space Station *Freedom*, extension of solar panels for augmenting the Orbiter's power (Solar Array Flight Experiment (SAFE)) and deployment of gigantic hoop column type antennae for mobile communications systems. NASA has also shown considerable interest in exploiting application of the Space Shuttle based tethered subsatellite systems and an experiment involving a 20 km long electrodynamic tether is scheduled for launch in 1992.

(iv) Attention is also directed towards planning of on-orbit experiments such as NASA Langley's Control Structure Interaction (CSI) program to check, calibrate and improve design algorithms. It is generally believed that on-orbit information acquired during the constructional phase of the Space Station is the only dependable procedure for its overall design. Obviously, this promises to open up an exciting area of in-flight parameter measurement techniques in structural dynamics, stability and control. With the commitment to an operational Space Station by the late 1990s, the need for understanding structural response characteristics and control strategies for such time varying, highly flexible systems is further emphasized.

One must recognize that flexibility is a design choice dictated in part by a dichotomy of extremes in the force field: very high accelerations during delivery to orbit followed by very low accelerations in the operational life. Generally, configuration size and weight are often severely constrained as a result of the launch vehicle limitations or structural strength of the system components. As as solution, spacecraft are initially stowed as compact rigid bodies. Once in orbit, various elements deploy to establish the prescribed configuration. In the case of the Space Station's construction, pre-assembled components will be deployed in orbit, thus changing the mass, inertia, flexibility and structural damping characteristics as their integration progresses. The presence of environmental and operational disturbances will only add to the complexity of the problem.

A question arises: why not conduct ground simulation studies before deploying a structure or its subassemblies in space? Ground based simulation studies for extremely flexible structures, with time dependent geometrical and structural properties, operating in a microgravity environment have proved to be of doubtful value. Accurate representations of the gravity field and other environmental forces have shown to be elusive. This has led to more reliance on mathematical modelling than in the past. Thus, the trend has been towards development of numerical tools which can be used with an increased level of confidence.

2 SCOPE OF THE INVESTIGATION

Having recognized the importance of flexibility, particularly with reference to large evolving space structures, there has been considerable effort aimed at general formulations applicable to a wide class of systems. The models considered vary significantly; however, the underlying objective is to obtain dynamic equations of motion for a system of arbitrarily connected flexible members in a branched or closed-loop topological form. Formulation procedures aimed at dynamics of multibody flexible spacecraft have been developed by several researchers. These include the early contribution by Ho[3] using the direct path method to more recent ones by Singh *et al.*[27] (Kane's approach), Meirovitch and Quinn[12] (perturbation technique), Vu-Quoc and Simo[31] (rotationally fixed floating frame approach), Spanos and Tsuha[29] (components modes method), Modi and coworkers[18,19] (Lagrangian approach), and others.

A comment concerning the Lagrangian approach to the problem may be appropriate. It has not been popular in multibody dynamics because the kinetic energy expression can become extremely lengthy and perhaps unmanageable (before the advent of high speed computers) as indicated by Hooker[5] and others. On the other hand, its effectiveness has been tested by a variety of problems in analytical dynamics for more than 200 years. More specifically, the approach automatically satisifes holonomic constraints. It provides expressions for useful functions such as Lagrangian, Hamiltonian, conjugate momenta, etc., and the form of the governing equations conveys a clear physical meaning in terms of contributing forces. Equally important is the fact that the equations are readily amenable to stability study and well suited for control design.

This paper presents a relatively general Lagrangian formulation of the nonlinear, nonautonomous and coupled differential equations of motion governing the dynamics of a system of interconnected structural members. The emphasis throughout is on the methodology of approach with details given in the references cited. The formulation has the following distinctive features:

(i) arbitrary number, type (five basic structural members and their combinations: tether, membrane, beam, plate and shell) and orientation of

flexible members, interconnected so as to form a topological configuration, deploying individual members independently at specified velocities and accelerations;

(ii) the appendage is permitted to have variable mass density, flexural rigidity and cross-sectional area along its length;

(iii) the governing equations account for gravitational effects, shifting center of mass, changing inertia and appendage offset (from the center of mass) together with transverse, axial and torsional oscillations; it also accounts for the solar radiation induced thermal deformations;

(iv) appendage as well as system rotations can be described using Euler and Rodrigues parameters, or any other orientation angles;

(v) to account for the flexible character of structural members in a consistent manner, a second-degree nonlinear displacement field is permitted. Alternatively, a linear displacement field can be used if the nonlinear terms up to the fourth degree are preserved in the strain energy expression;

(vi) elastic deformations can be discretized using modal representation, admissible functions, finite elements, or lumped mass method;

(vii) joints between the flexible members are taken to be elastic and dissipative permitting relative rotation and translation between the structural members;

(viii) the system may contain momentum or reaction wheels, gimbaled or fixed, as well as thrusters;

(ix) in spacecraft dynamics studies, the generalized coordinates corresponding to librational degrees of freedom can be so chosen as to make the governing equations applicable to both spin stabilized and gravity gradient orientations;

(x) the equations are programmed in nonlinear as well as linear form to permit the study of:
- large angle manoeuvers;
- nonlinear effects;
- control strategies.

The computer code is written in a modular fashion to help isolate the effects of flexibility, deployment, character and orientation of the appendages, inertia and orbital parameters, number and type of admissible functions, etc. Environmental effects due to solar radiation, aerodynamic forces, earth's magnetic field, etc., can be incorporated easily through generalized forces. The same is true for internal and external dissipation mechanisms.

3 FORMULATION OF THE PROBLEM

3.1 System geometry

The system model selected for study consists of an arbitrary number of flexible bodies connected to form a branched geometry: central body B_c is connected to bodies B_i ($B_1, \ldots, B_N$). In turn, each B_i is connected to $B_{i,j}$ bodies ($B_{i,1} \ldots, B_{i,n_i}$) as shown in Fig. 1. Altogether, there are $N_{i,j}$ ($= \sum_{i=1}^{N} n_i$) number of $B_{i,j}$ bodies. Thus, the total number of interconnected structural members amounts to $N+N_{i,j}$.

It should be noted that the number and locations of bodies are kept arbitrary so that the configuration can be used to study a large and varied class of future spacecraft including the proposed Space Station *Freedom*. For instance, the European Space Agency's L-SAT (large satellite system, Olympus) represents a new generation of communications satellite. It has two solar panels connected to a central body. The satellite's central rigid body and two solar panels can be simulated by bodies B_c and B_i, respectively. In the case of the Space Station, the power boom can be represented by the central body B_c while the modules, radiators, stinger, α and β joints can be modelled by B_i bodies. $B_{i,j}$ bodies may constitute the solar panels.

3.2 Equations of motion

Some of the details of the Lagrangian formulation have been reported earlier.[19] Further information can be found in the doctoral thesis by Ng.[24] Using the Lagrangian procedure, the governing equations of motion can be obtained from:

$$\frac{\mathrm{d}}{\mathrm{d}t}\left(\frac{\partial T}{\partial \dot{\bar{q}}}\right)-\frac{\partial T}{\partial \bar{q}}+\frac{\partial U}{\partial \bar{q}}=\bar{F}_q$$

where $\bar{q}$ and $\bar{F}_q$ represent the generalized coordinates and associated forces, respectively. The above equations can be rewritten in vector form as:

$$[M(\bar{q})]\,\ddot{\bar{q}}+[K(\bar{q})]\,\bar{q}=\begin{Bmatrix}\bar{G}_\theta\\ \bar{G}_p\end{Bmatrix}$$

where $[M(\bar{q})]$ and $[K(\bar{q})]$ represent the nonlinear mass and stiffness matrices, respectively, while $\bar{G}_\theta$ and $\bar{G}_p$ correspond to the nonlinear gyroscopic terms for the librational and vibrational degrees of freedom, respectively; $\bar{q}$ is comprised of two vectors, $\bar{\theta}$ and $\bar{\mathbf{p}}$, where $\bar{\theta}=\{\psi,\phi,\lambda\}$ for the librational degrees of freedom and $\bar{\mathbf{p}}=\{p_1,p_2,\ldots,p_n\}$ for the vibrational degrees of freedom.

Discretization of the physical system can be performed in two ways:

(i) In the component mode method, the number of

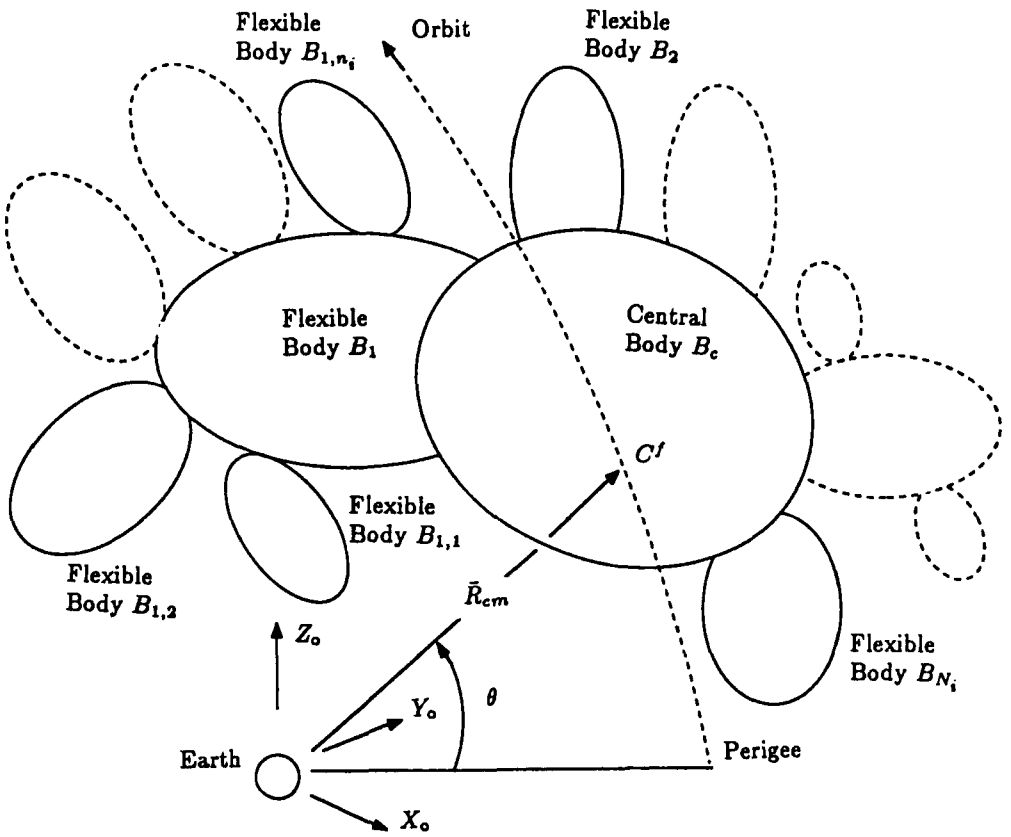

Fig. 1. A schematic diagram representing a wide class of systems composed of flexible interconnected bodies forming the tree type topology.

generalized coordinates depends on the system configuration, i.e. the degrees of freedom involved (for holonomic systems). For instance, consider a beam type central body B_c undergoing general librational motion with N beams (body B_i) attached to it. In turn, each B_i body is attached to n plate type members ($B_{i,j}$ bodies). Assuming m modes to represent flexural deformation for each of the flexible members, the total number of generalized coordinates is given by $N_q = 5+m+(N\times m)+(N\times n\times m)$.

(ii) In the system mode method, the number of generalized coordinates depend on the number of modes considered in the discretization of the continuum motion and not on the complexity of the system configuration. For instance, if one accounts for the m system modes to represent the flexibility of the model, the total number of generalized coordinate is given by $N_q = 5+m$.

In general, the effect of librational and vibrational motions on the orbital dynamics is small unless the system dimension are comparable to R_{cm}.[13] Hence, the orbit can be represented by the classical Keplerian relations:

$$R_{cm} = \frac{h^2}{\mu_e(1+\varepsilon\cos\theta)} \qquad R_{cm}^2\dot{\theta} = h$$

where h is the angular momentum per unit mass of the system, ε is the eccentricity of the orbit and θ is the true anomaly. μ_e represents the Earth's gravitational constant.

4 MODAL ANALYSIS

As pointed out before, the system under consideration may be of a transient and evolutionary character. Thus, the mathematical model would require freedom and ease with which system parameters such as geometry, flexibility and inertia can be varied. To this end, the finite element approach appears quite attractive because of the following reasons:

(i) The admissible functions are quite simple (low degree polynomials) and computationally desirable. Integrals involving such polynomials can be

evaluated in closed-forms, thus eliminating errors that may result from numerical integration.

(ii) Even for a complex flexible structure like the Space Station, system modes can be obtained quite readily. Moreover, the nodal feature of the finite element method makes handling of the boundary conditions straightforward.

(iii) The formulation is not affected by the evolving design. Once characteristics of the system are identified, a finite element that properly accounts for the physical properties is developed. Contribution of this element in the system's dynamical analysis is automatically accounted for in the assembly process. When a different structural configuration is encountered, say during the integration of a solar panel with the power boom, a new mesh layout and subsequent reassembly of the structure is all that is required.

Design of lattice structures, which constitute basic components of space systems, must be highly reliable since they cannot be tested full scale in their operational environments prior to the flight. Even a scale model of the structure can be tested in the ground based environmental chambers only in an approximate manner. This is because of the practical difficulty in reproducing gravity gradient, free molecular, magnetic, plasma and solar radiation effects, as pointed out before.

On the other hand, a detailed finite element analysis of these members would involve a large number of elements and nodes, thus becoming uneconomical, especially in the initial design phase when the structure and its associated systems are subject to modifications. At the same time, the structure's high flexibility may require a relatively large number of elastic modes to be accurately predicted. The control analyst may also require accurate estimate of the structure's high frequency modes rather than just those at low frequencies.

Procedures for modelling large truss structures by means of equivalent continuous systems have been developed by Berry *et al.*[1] and Juang and Sun.[8] Their studies suggest the necessity to model large truss structures by the geometrically nonlinear Timoshenko beams. While shear and rotary inertia lead to small corrections to the Bernoulli–Euler theory for the lower modes of long, thin beams, significant errors may be introduced if they are neglected when dealing with thicker beams, or for the higher modes of any beam.

A number of Timoshenko beam type finite elements have been proposed in the literature.[21] They can be divided into two classes: simple and complex. A simple element has a total of four degrees of freedom, two at each of the two nodes, for unidirectional bending in a principal plane. A complex element has more than four degrees of freedom, i.e. more than two degrees of freedom at a node or more than two nodes. The nodal variables usually used are transverse displacement, shear deformation and the rotation of the cross-section.

The simple element has been selected in the present study. It is well suited for the analysis of complex structures, since the nodal variables are cross-section rotations and transverse displacements. The element was found to have a good rate of convergence.

4.1 Typical results for evolving Space Station configurations

Effectiveness of the finite element program for determining system modes was assessed through its application to a highly complex and flexible system, the proposed Space Station.

The Space Station *Freedom* is planned to be assembled in orbit utilizing around 30 space transportation system (STS) flights.[23] Essentially it consists of the main truss (power-boom), 155 m long, with the pressurized modules (Habitation, Laboratory and Logistics) located near the geometric center of the spacecraft. Servicing equipment will be placed along the power-boom on either side of the cluster of modules. Ends of the main truss will support four photovoltaic arrays, each 33 m in length, to deliver 75 kW of power from conventional solar cells.

The first 40 system modes for four intermediate configurations of the evolving Space Station were obtained. The first element launch (MB-1, Fig. 2(a)) consists of a 25 m long boom, a 11·5 m long array radiator (both modelled as beams) and a pair of solar panels (33 m × 6 m × 0·25 m) represented as plates. During the second Shuttle flight (MB-2 configuration) the main truss is extended to 55 m and an additional station radiator (10 m × 5 m × 0·25 m) is attached to it. The transition from the MB-2 to MB-3 configuration involves incorporation of a lumped mass element at the lower end of the main truss representing the module support structure and pressurized docking adapter (25000 kg). Finally, the permanently manned configuration (PMC), completed at the end of the twentieth Shuttle flight (Fig. 2(b)), has a 115 m main truss with a module cluster at its geometric centre (146000 kg); a pair of array and station radiators located at 40 and 21 m from the truss center, respectively; and solar arrays near each end of the truss. The process continues until the complete Space Station is integrated by the end of the thirtieth flight. For conciseness only the frequency spectra for the beginning MB-1 and the final PMC stages are presented here (Fig. 3). It is of interest to point out that there are 24 modes (besides the rigid body modes) below 5 Hz for the MB-1 configuration! For example, the first elastic mode represents the arrays' fundamental bending (symmetric)

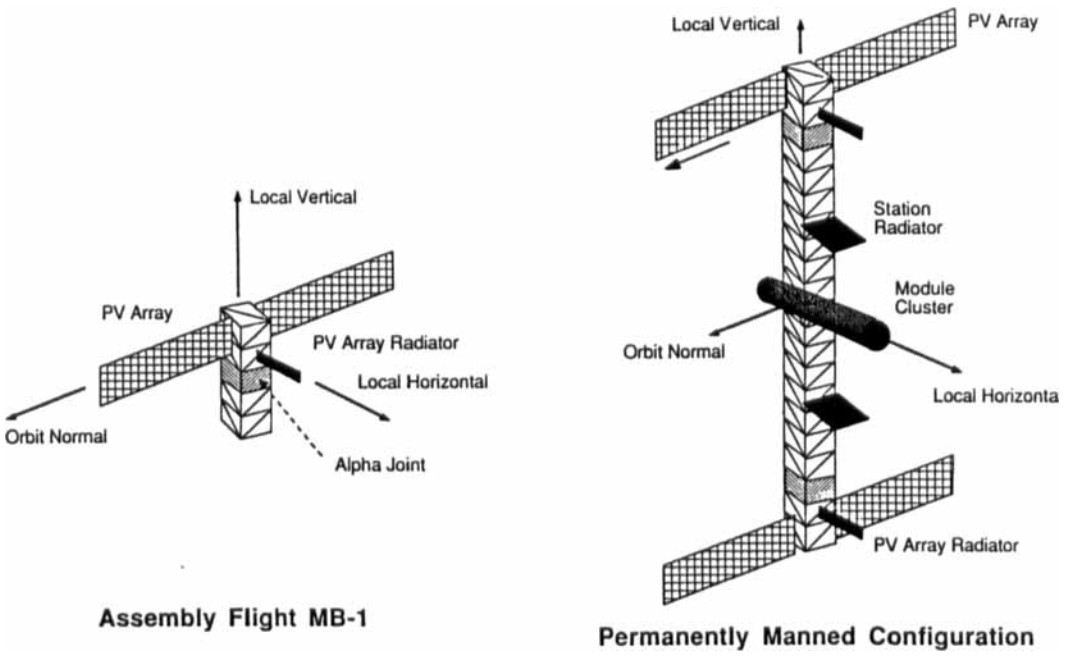

Fig. 2. The Space Station *Freedom*'s assembly sequence showing two of the evolutionary phases.

(a)

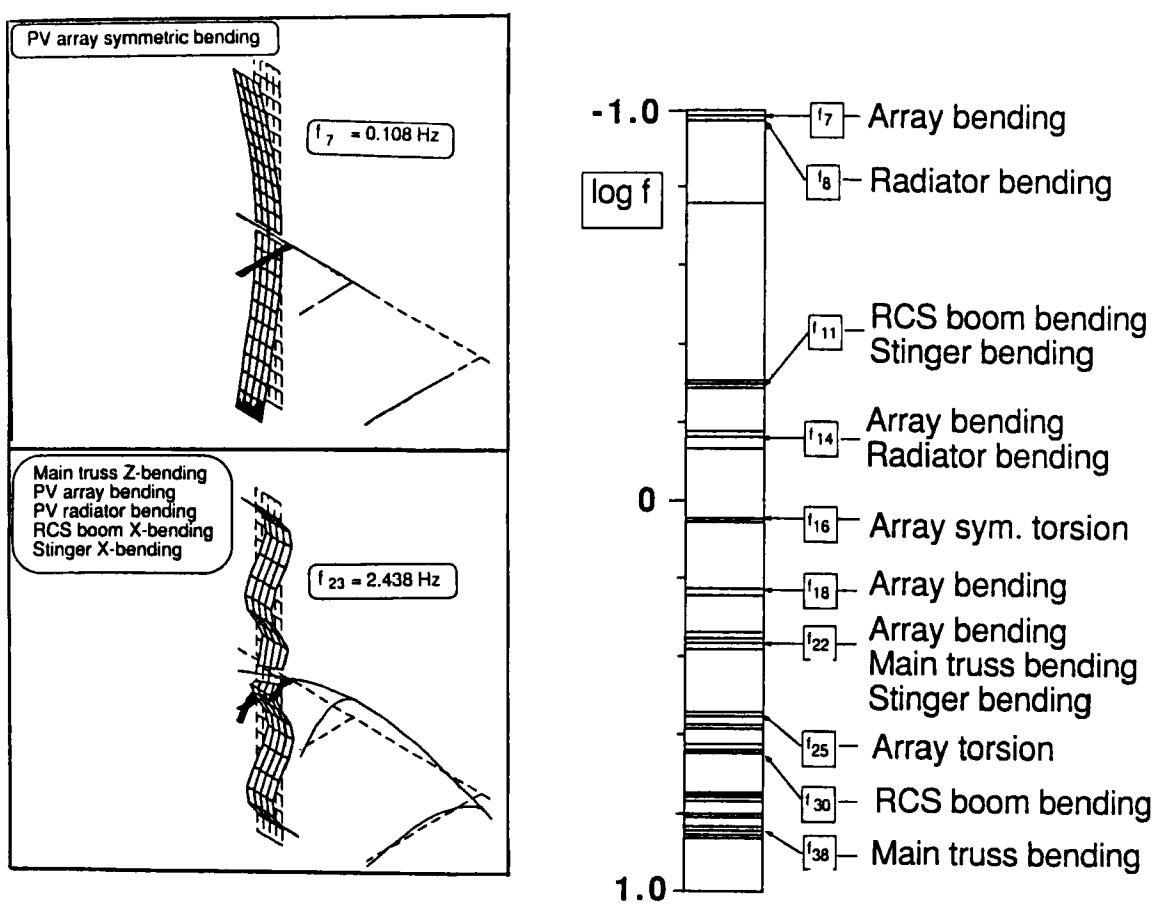

Fig. 3. Frequency spectra and representative modes for two intermediate configurations of the evolving Space Station *Freedom*: (a) first flight (MB-1).

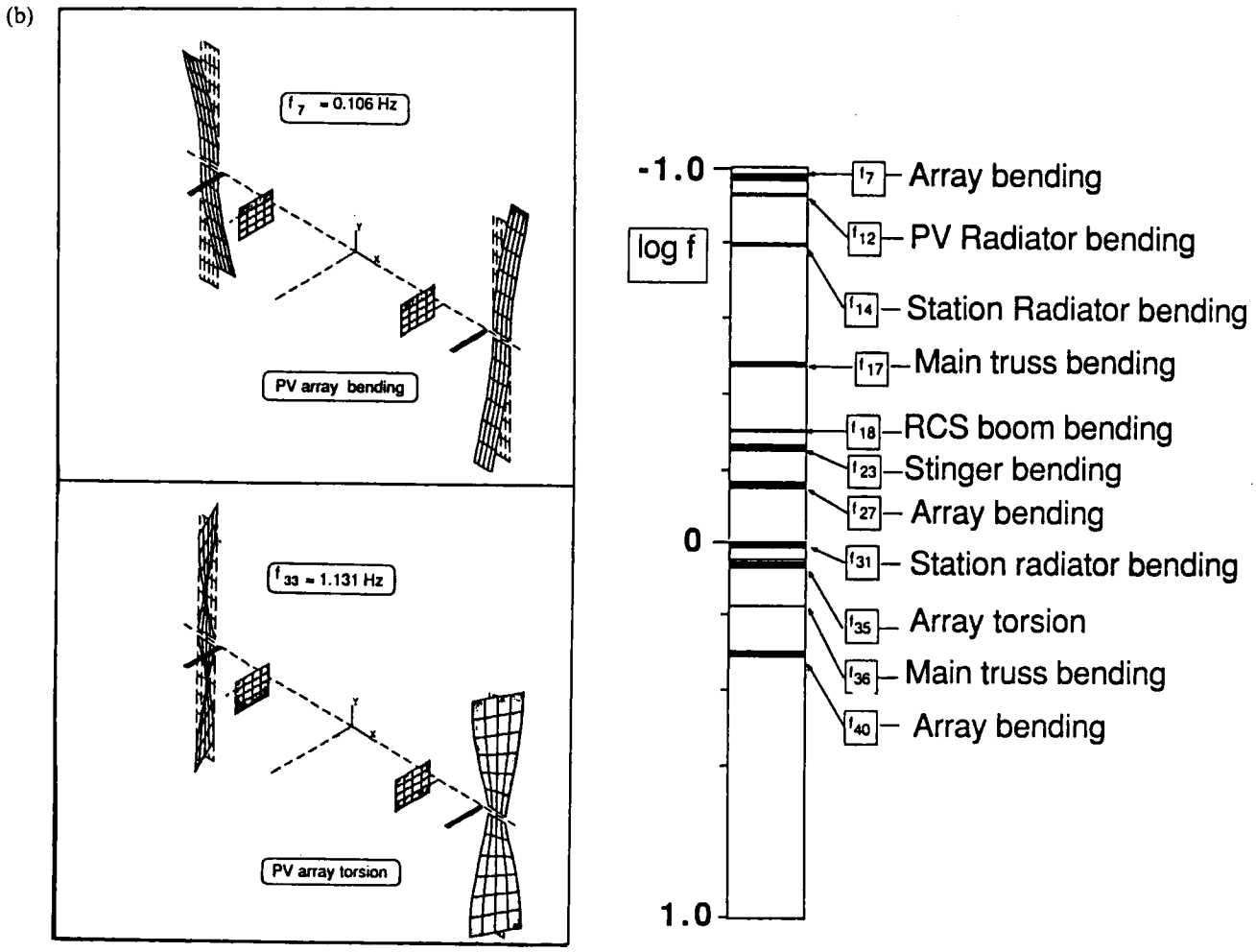

Fig. 3.—*contd.* (b) Permanently manned configuration (PMC).

at around 0·1 Hz. Predominantly $f_{10} = 0{\cdot}5$ Hz is the RCS boom and the stinger bending mode. The main truss first bending mode occurs at $f_{21} = 2{\cdot}3$ Hz. For the PMC case, both the length as well as the system weight have increased. This leads to more modes in a given frequency range. Now the lowest bending modes for the truss correspond to $f_{17} = 0{\cdot}32$ Hz and $f_{20} = 0{\cdot}35$ Hz.

Summarizing, it can be inferred that the appendages dominate the flexible dynamics and modes involving their pure motion are not significantly affected by the evolutionary character of the Space Station. However, growth of the main truss and its interaction with the cluster of modules significantly affect the system modes as observed through the changes in the truss bending frequencies.

5 APPROACH TO NUMERICAL SIMULATIONS

Several general purpose computer codes aimed at studying dynamics of multibody systems have been commercially available for some time. They include DISCOS,[2] ALLFLEX,[4] TREETOPS[27] and SD/FAST.[28] Primarily they are suitable for systems with large rigid body motion with flexible members undergoing small deformations. As expected, each asserts a variety of distinctive and desirable features and they have been used extensively with a varying degree of success often governed by the nature of the system, experience of the user and computational tools available. In general, they present a scope for improvement in representation of axial foreshortening leading to dynamic stiffness effects, rotary inertia and shear deformation. Furthermore, it is widely recognized that:

(i) rendering the program operational often demands enormous time and effort;
(ii) user-end modification and adaptability of the program is often very cumbersome if not impossible;
(iii) contribution of the various forces and moments to the governing equations of motion is usually

not available explicitly making analysis of results and physical appreciation of the system dynamics difficult;

(iv) general character of the formulation and computational methodology applied leads to nonoptimum numerical performance when dealing with relatively simple system configurations.

Here, a general purpose computer program has been developed based on the formulation presented in Section 3. The flowchart for the program is shown in Fig. 4. Essentially, it can be divided into two parts: input and numerical integration. In the input phase, the user is required to supply information, including:

(i) orbital elements such as eccentricity;
(ii) the topology of the system tree;
(iii) the individual substructure physical properties such as mass, length, inertia, location, and orientation;
(iv) inclusion/exclusion of the environmental effects;
(v) simulation period and the numerical integration subroutine parameters such as accuracy, integration method, etc;
(vi) initial conditions representing disturbances.

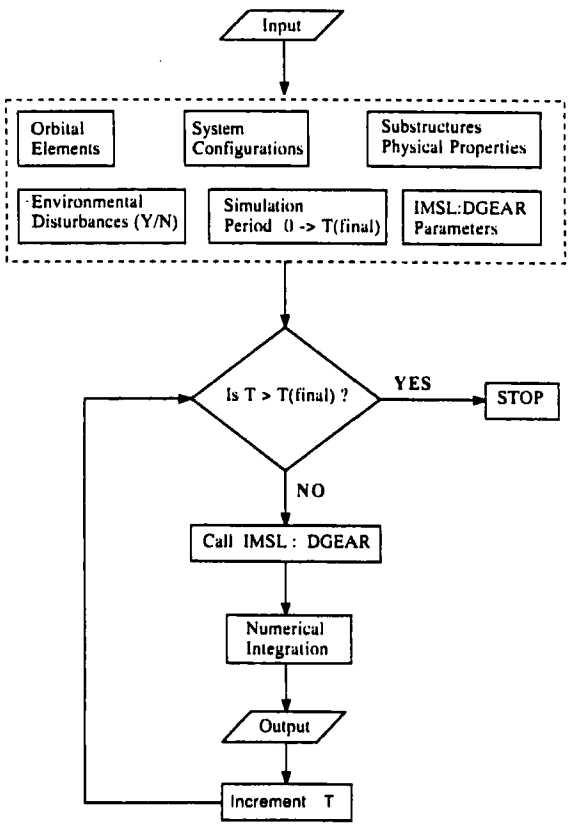

Fig. 4. Flowchart of the computer program for the general formulation.

With this information in hand, the numerical integration phase begins. The IMSL:DGEAR[6] subroutine is chosen for its robustness and capability to integrate both stiff and nonstiff equations efficiently. The structure of the numerical integration part is divided into subroutines, each responsible for different aspects of the computation, such as modal integrals, inertias, angular momentum, kinetic and potential energies, generalized forces, assembly of equations of motion, control and so on. The modular structure permits user end modification of the program with relative ease. For instance, if one wants to investigate the effect of aerodynamic drag, modification of the generalized force subroutine is all that is required. The rest of the program remains intact. The program, written in Fortran, is small in size (< 2 MB); hence, it can be executed either on a workstation or in a mainframe environment.

The relatively general character of the governing equations made it possible to study dynamics and control of a wide variety of systems including: (i) an arbitrary satellite deploying thermally flexed gravity gradient booms; (ii) the Space Shuttle based slewing mast with a reflector plate type antenna once proposed in the Structural Control Laboratory Experiment (SCOLE); (iii) evolving structures, like the proposed Space Station, with time dependent geometry, inertia, flexural rigidity, damping, and other structural properties; (iv) the space platform based tethered satellite system during deployment, station-keeping and retrieval; (v) flexible, mobile orbiting manipulator, traversing a flexible platform and supporting an elastic payload; to name a few. For conciseness, the objective here is limited to illustrating its versatility through application to only two systems of contemporary interest.

6 NUMERICAL SIMULATION OF THE PMC

A relatively simple yet effective dynamic model of the permanently manned configuration of the Space Station is shown in Fig. 5. Here, the PMC is idealized as one free–free beam (power-boom), cantilever beam (stinger), and eight cantilever plates (four PV arrays, two PV array radiators and two station radiators). The physical properties, obtained from the NASA *Space Station Engineering Data Book*,[22] are summarized in Table 1. Using the component mode method and considering only the first mode of vibration for each member, there are altogether 15 generalized coordinates. They include the librational degrees of freedom: pitch (ψ), roll (ϕ) and yaw (λ). Two generalized coordinates are necessary to describe the power boom vibration in the local vertical and horizontal direction (δ_c^y, δ_c^z). Similarly, the stinger vibration in the local vertical and orbit normal direction

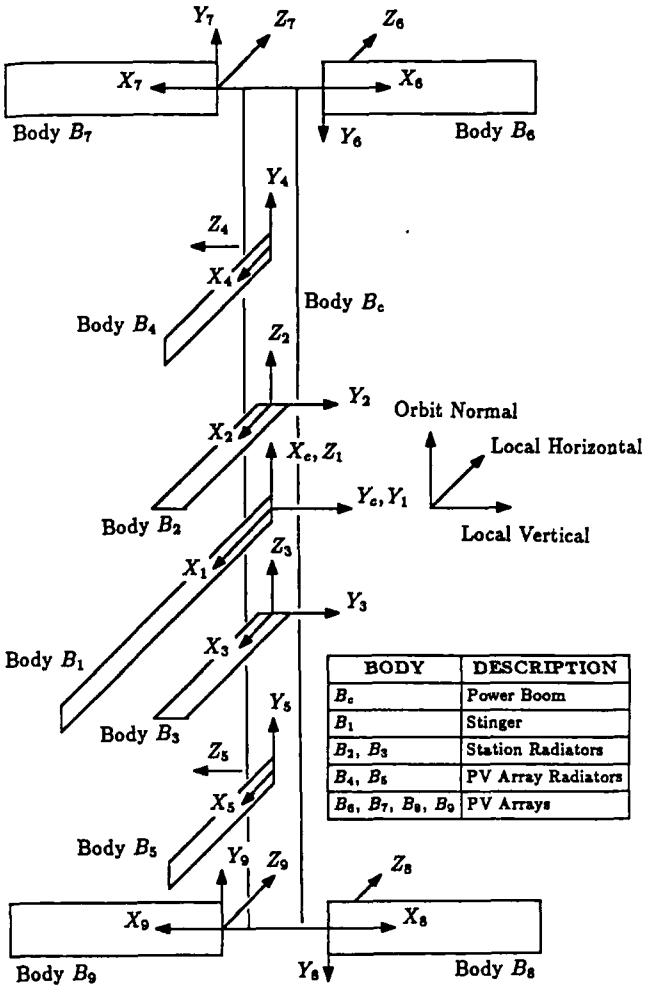

Fig. 5. Configuration of the PMC and associated coordinate systems.

are represented by δ_1^y and δ_1^z, respectively. The elastic deformations of the station radiators in the orbit normal direction are denoted by the generalized coordinates ε_2^x and ε_3^x for B_2 and B_3, respectively. The vibration of the PV array radiators, which is in the local vertical direction, is denoted by ε_4^x and ε_5^x. Finally, the PV array deflections in the local horizontal direction are represented by ε_6^x, ε_7^x, ε_8^x and ε_9^x. The generalized coordinate vector $\bar{\mathbf{q}}$ can therefore be written as:

$$\bar{\mathbf{q}} = [\psi, \phi, \lambda, \delta_c^y, \delta_c^z, \delta_1^y, \delta_1^z, \varepsilon_2^x, \varepsilon_3^x, \varepsilon_4^x, \varepsilon_5^x, \varepsilon_6^x, \varepsilon_7^x, \varepsilon_8^x, \varepsilon_9^x]^T$$

6.1 Dynamical response

To begin with, Fig. 6 shows the system response when the power boom initially deformed in the first mode with a tip deflection of 1 cm. For the initial deflection in the local vertical direction, Fig. 6(a) shows the system response over 0·02 orbit. The power boom disturbance in the local vertical direction excites the pitch libration motion with high frequency harmonics. The stinger, though excited, vibrates predominantly in the local vertical direction (δ_1^y) with a magnitude of 0·6 cm peak-to-peak. Other flexible components oscillate with frequencies of the power boom. Even with this small initial condition, PV array radiators experience a large deflection (ε_4^x) with a peak amplitude of 2·5 cm. In Fig. 6(b), the response of the PMC is due to an initial disturbance in the local horizontal direction. Now the pitch response is negligible, so are the stinger and the PV array radiator motions with peak amplitudes of 0·01 cm (δ_1^y) and 0·1 cm (ε_4^x), respectively. It is interesting to note that both the station radiators (ε_2^x) and the PV arrays (ε_6^x) have an identical response trend but of different amplitudes: 1 cm for the station radiators and 2·5 cm for the PV arrays, although the latter is more massive.

The focus is now turned to the stinger disturbance. With the stinger tip initially displaced by 1 cm in the local vertical direction, Fig. 7(a) shows that the PMC is undergoing low amplitude but high frequency oscillations about the orbit normal (ψ). The power boom, PV array and radiator respond with maximum amplitudes of 0·003 cm (δ_c^y), 0·1 cm (ε_6^x) and 0·05 cm (ε_4^x), respectively. Note that the stinger response in the orbit normal direction (δ_1^z) is negligible. The response of the PMC with initial stinger disturbance in the orbit normal direction is shown in Fig. 7(b). Note that, as before, the pitch degree of freedom is virtually unexcited; however, the roll and yaw responses are significant. The power boom and the stinger deformation in the local vertical direction (δ_c^y, δ_1^y) are rather small. The amplitudes of the PV array and radiator are indeed small with a maximum array displacement (ε_6^x) of only 0·01 cm.

6·2 Velocities and accelerations

One of the stated missions of the Space Station is to provide a microgravity environment for the purpose of scientific research. As stated in the NASA report,[22] the objective of the station is to create 1–10 μg environment in some portion of the laboratory module. Furthermore, a drift rate, apart from the orbital rate ($\dot{\theta}$), below 0·005°/s ($0{\cdot}872 \times 10^{-4}$ rad/s) is desired. Using the data obtained for Figs 6 and 7, variations of angular velocities ($\omega_x, \omega_y, \omega_z$), angular accelerations ($\alpha_x, \alpha_y, \alpha_z$) and power boom accelerations (a_c^y, a_c^z) about the X_c, Y_c, Z_c-axes are plotted. The angular accelerations which are expressed as μg/m can be interpreted as the μg level at 1 m from O_c, the origin of the X_c, Y_c, Z_c-axes. For instance, $\alpha_x = 1$ μg/m implies that a point 1 m on the Y_c- or Z_c-axis experiences an acceleration of 1 μg due to the angular acceleration about the X_c-axis. Assuming the microgravity experiment workspace to be about 10 m from O_c, a 1–10 μg/m environment would therefore require

Table 1
System parameters used in the numerical simulation of the PMC

Power boom (Body B_c)
$l_c = 115$ m
$m_c = 154583$ kg
$\omega_c^1 = 0{\cdot}193$ Hz
$(I_{xx})_c = 1{\cdot}44 \times 10^6$ kg m^2
$(I_{yy})_c = 43{\cdot}26 \times 10^6$ kg m^2
$(I_{zz})_c = 43{\cdot}26 \times 10^6$ kg m^2
$(I_{xz})_c = 0{\cdot}18 \times 10^5$ kg m^2

Stinger (Body B_1)
$l_1 = 26{\cdot}7$ m
$m_1 = 270$ kg
$\omega_1^1 = 0{\cdot}5$ Hz
$(I_{xx})_1 = 3844$ kg m^2
$(I_{yy})_1 = 64160$ kg m^2
$(I_{zz})_1 = 64160$ kg m^2

Station radiator (Body B_i, $i = 2,3$)
$l_i = 11{\cdot}5\ m$
$m_i = 1395$ kg
$\omega_i^{1,1} = 0{\cdot}1\ Hz$
$(I_{xx})_i \approx 0$
$(I_{yy})_i = 61496$ kg m^2
$(I_{zz})_i = 65340$ kg m^2

PV radiator (Body B_i, $i = 4,5$)
$l_i = 11{\cdot}5$ m
$m_i = 450$ kg
$\omega_i^{1,1} = 0{\cdot}1$ Hz
$(I_{xx})_i = 50$ kg m^2
$(I_{yy})_i = 19837$ kg m^2
$(I_{zz})_i = 19887$ kg m^2

PV array (Body B_i, $i = 6,\ldots 9$)
$l_i = 33$ m
$m_i = 444$ kg
$\omega_i^{1,1} = 0{\cdot}1$ Hz
$(I_{xx})_i = 1332$ kg m^2
$(I_{yy})_i = 161172$ kg m^2
$(I_{zz})_i = 162504$ kg m^2

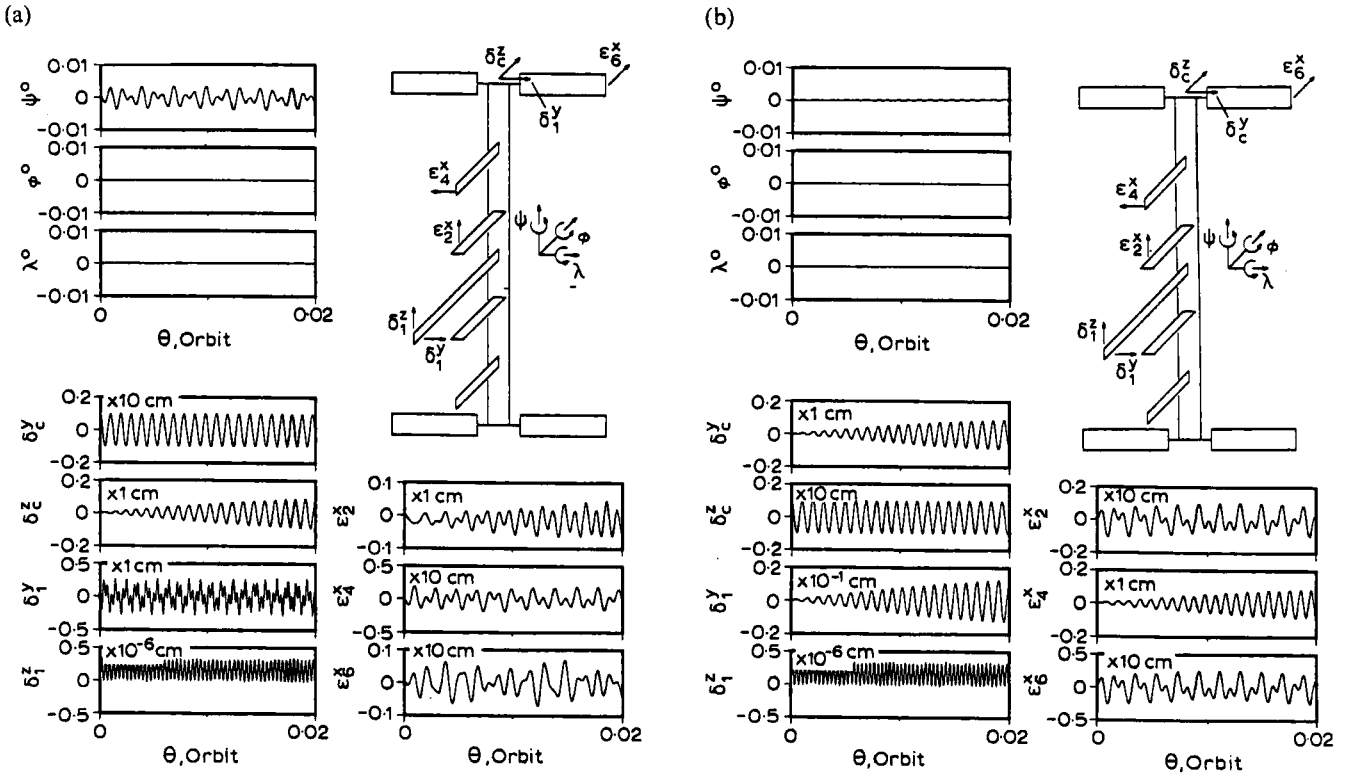

Fig. 6. The influence of the power boom initial tip displacement of 1 cm on the PMC response: (a) initial displacement in the local vertical direction. (b) Initial displacement in the local horizontal direction.

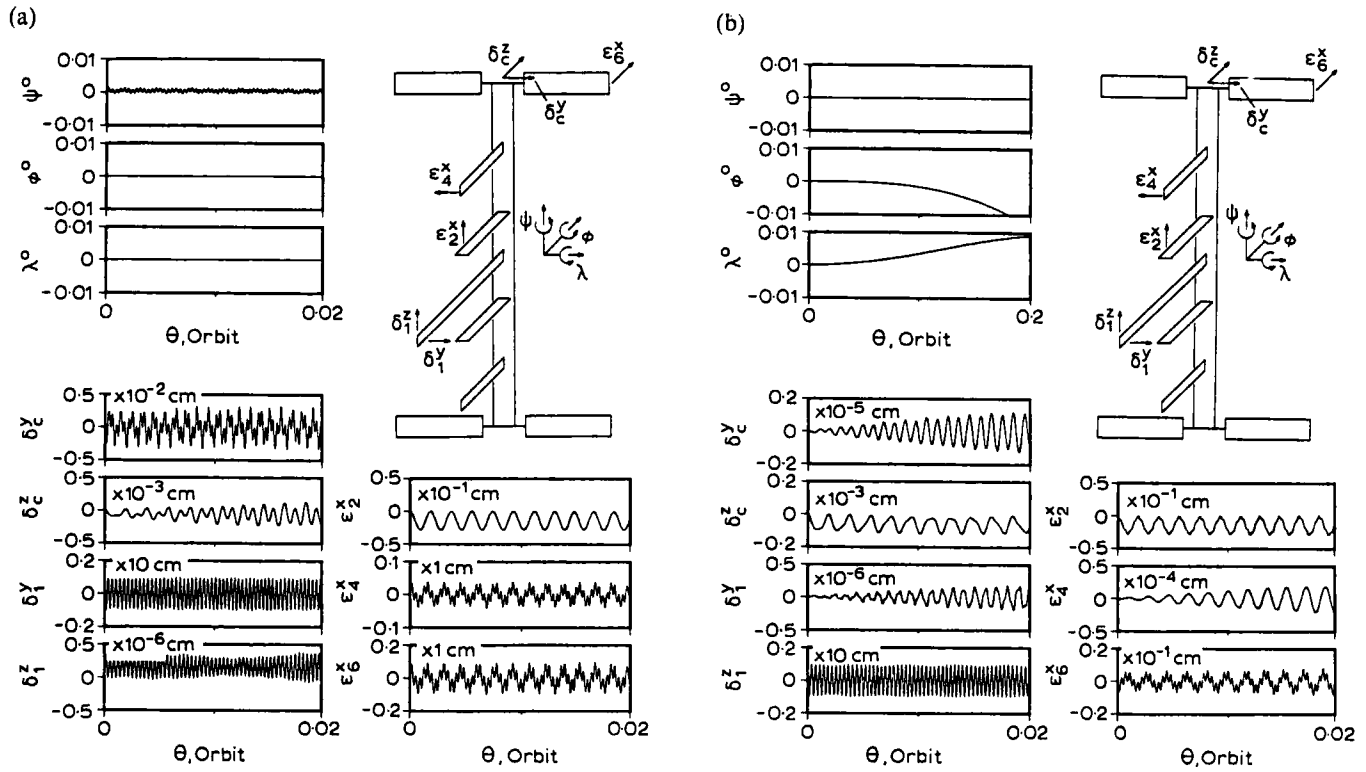

Fig. 7. Response of the PMC subjected to an initial 1 cm tip deflection of the stinger: (a) initial deflection in the local vertical direction. (b) Initial deflection in the orbit normal direction.

the angular acceleration about any axis to be less than 1 μg/m. Finally, the power boom accelerations are presented in terms of μg.

Figure 8 illustrates the velocity and acceleration variations for the PMC subjected to an initial power boom disturbance. Figure 8(a) corresponds to the case shown in Fig. 6(a), where the power boom is initially given 1 cm tip deflection in the local vertical direction. Even with such a small disturbance, the resulting angular velocities and accelerations approach or exceed the specified limit. For instance, maximum ω_x and α_x attain values of 0·004°/s and 500 μg/m, respectively. The microgravity level near the power boom center is over 1000 μg. With the initial disturbance applied in the local horizontal direction, the magnitudes of both velocities and accelerations are about an order of magnitude smaller (Fig. 8(b)); however, the accelerations still exceed the design limit. Once again, the angular velocity and acceleration about the X_c-axis are largest with magnitudes of 2×10^{-4} °/s and 10 μg/m, respectively. The boom acceleration results in a microgravity level exceeding 1000 μg in the local horizontal direction. Figure 7 shows that the influence of the stinger disturbance on the PMC response is small; hence, it is reasonable to predict that angular velocities and accelerations to be small. The prediction is correct; however, they are not negligible when the disturbance is applied in the local vertical direction. Under this condition, Fig. 9(a) illustrates that the maximum drift rate is 0·0025 °/s about the X_c-axis but the maximum angular acceleration has an amplitude of 300 μg/m about the Y_c-axis. The microgravity level due to the boom accelerations reaches a value of 6 μg in the local vertical direction. When the same stinger disturbance is applied in the out-of-plane direction, both the velocities and accelerations stay within the limit (Fig. 9(b)). Now, the maximum angular velocity ($0{\cdot}3 \times 10^{-6}$ °/s) and acceleration (0·01 μg/m) are about the Z_c-axis while the boom vibration results in a 0·02 μg acceleration.

The results of Figs 8 and 9 provide valuable information pertaining to the velocities and microgravity environment of the PMC. The results indicate that the requirements on velocity and acceleration are stringent. Even with a small disturbance applied to the power boom or stinger, the system velocities and accelerations easily reach or exceed the design limit. The information is fundamental to the design of an appropriate control system.

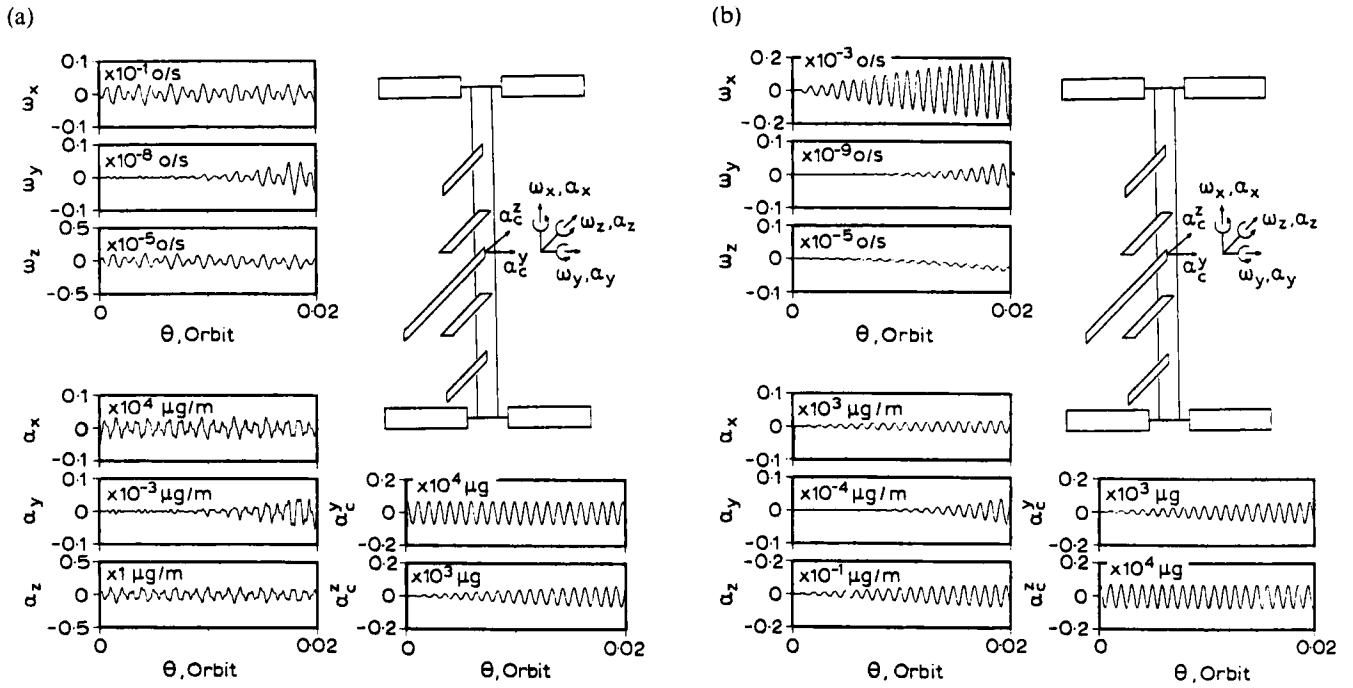

Fig. 8. The effect of the power boom disturbance on the PMC velocities and accelerations: (a) initial power boom tip displacement of 1 cm in the local vertical direction. (b) Initial power boom tip displacement of 1 cm in the local horizontal direction.

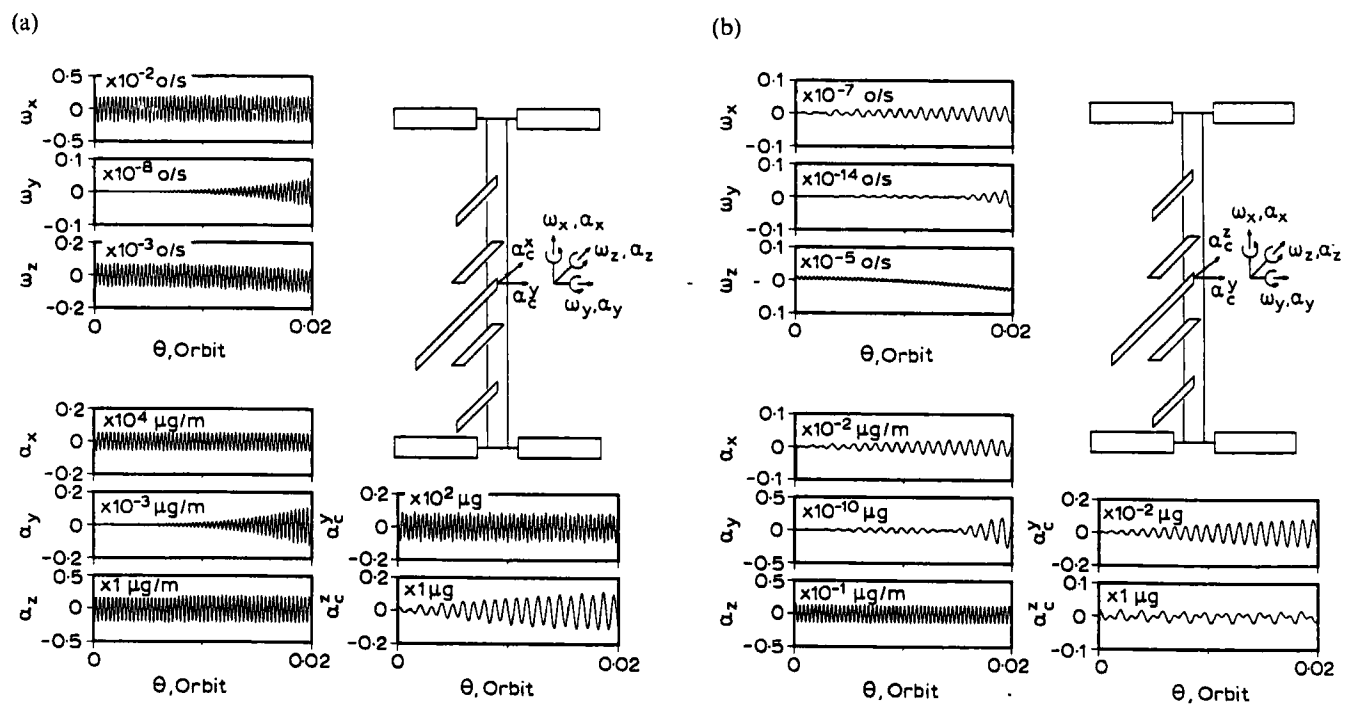

Fig. 9. The effect of the stinger disturbance on the PMC velocities and accelerations: (a) initial stinger tip displacement of 1 cm in the local vertical direction. (b) Initial stinger tip displacement of 1 cm in the orbital normal direction.

Table 2
System parameters used in the numerical simulation of SFU

Before deployment	*After deployment*
Main body (Body B_c)	
$l_c = 4{\cdot}9$	4·9 m
$m_c = 3964{\cdot}8$	3886 kg
$(I_{xx})_c = 7839{\cdot}2$	7524 kg m^2
$(I_{yy})_c = 4410{\cdot}0$	4410·0 kg m^2
$(I_{zz})_c = 6079{\cdot}2$	5764 kg m^2
Solar array pedal (Body $B_i, i = 1,2$)	
$l_i = 3$	9·7 m
$m_i = 17{\cdot}6$	57 kg
$\omega_1^i = 1{\cdot}934$	0·185 Hz
$(I_{xx})_i = 20$	20 kg m^2
$(I_{yy})_i = 68{\cdot}7$	2321 kg m^2
$(I_{zz})_i) = 69$	2331 kg m^2

7 NUMERICAL SIMULATION OF THE SFU

The space flyer unit (SFU) is an unmanned, reusable and free-flying platform for multipurpose use. The SFU is developed by a consortium of Japanese government agencies including the Institute of Space and Astronautical Science.[28] The unit is scheduled to be launched in early 1993. The SFU consists of an octagonal-shaped central body which includes eight modules of scientific experiments. Two solar array pedals (SAPs), each 9·7 m × 2·4 m, are deployed at either end of the central body. The SAPs, besides generating power, are used for the high voltage solar array (HVSA) experiment aimed at investigating:

(i) the dynamical characteristics of the unit during the deployment and retrieval of the flexible SAPs;
(ii) the upper limit of the voltage generated which would be free from surface breakdown, power drain through space plasma, and enhancement of the aerodynamic drag.

Here, the present formulation is used to simulate the dynamics of the SFU during deployment and retrieval of the pedals accounting for the time dependent system properties.

The unit is idealized as a rigid central body (B_c) with two deployable cantilevered plates (B_1 and B_2). Assuming a 90 min orbit, the simulation is based on the data in Table 2 and the coordinate systems as shown in Fig. 10. Note that the spacecraft can assume either one of the two orientations. In the first orientation, the SAPs have their longitudinal axes along the orbit normal whereas in the second case, the axes are aligned with the local vertical.

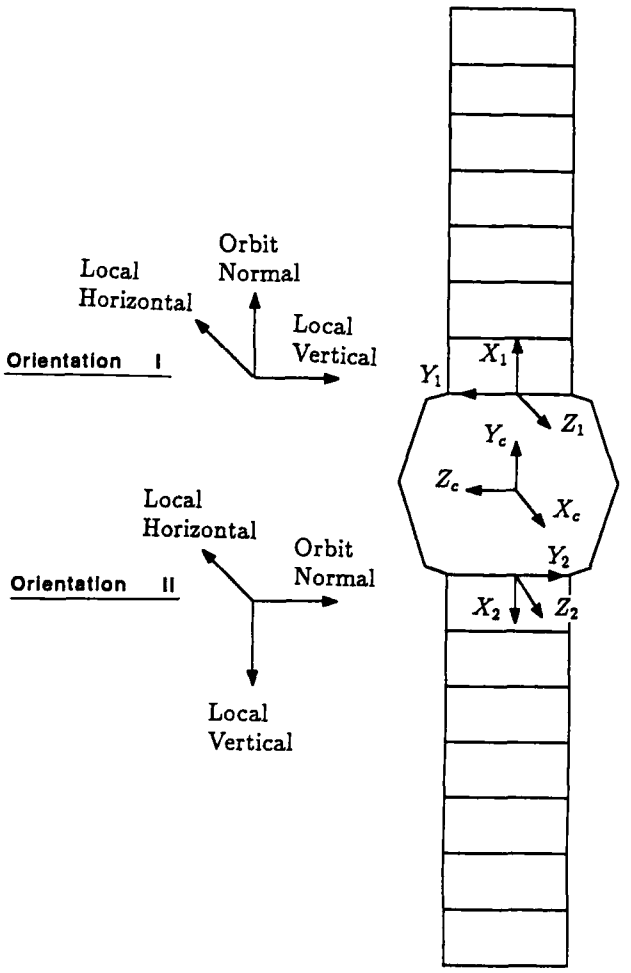

Fig. 10. Configuration of the SFU and associated coordinate systems.

Considering only the first mode of SAP vibration, the generalized coordinate vector would consist of five elements. Three correspond to the librational degrees of freedom: pitch (ψ), roll (ϕ) and yaw (λ); while two are associated with the vibration modes ($\varepsilon_1^r, \varepsilon_2^r$) for B_1 and B_2, respectively:

$$\bar{\mathbf{q}} = [\psi, \phi, \lambda, \varepsilon_1^r, \varepsilon_2^r]^T$$

The same parameter values are used for the retrieval study except that the two columns of data are interchanged. For instance, the length of the SAP before and after retrieval would be 9.7 and 3 m, respectively. Ideally, simulations should be based on the SAP length from 0 to 9·7 m. However, this would make the governing equations of motion extremely stiff initially and hence a considerable amount of computational effort would be required. It is therefore assumed that the pedal remains rigid until 3 m of deployment. Even with this simplification, the natural frequency of the array would reach a high of 1·93 Hz.

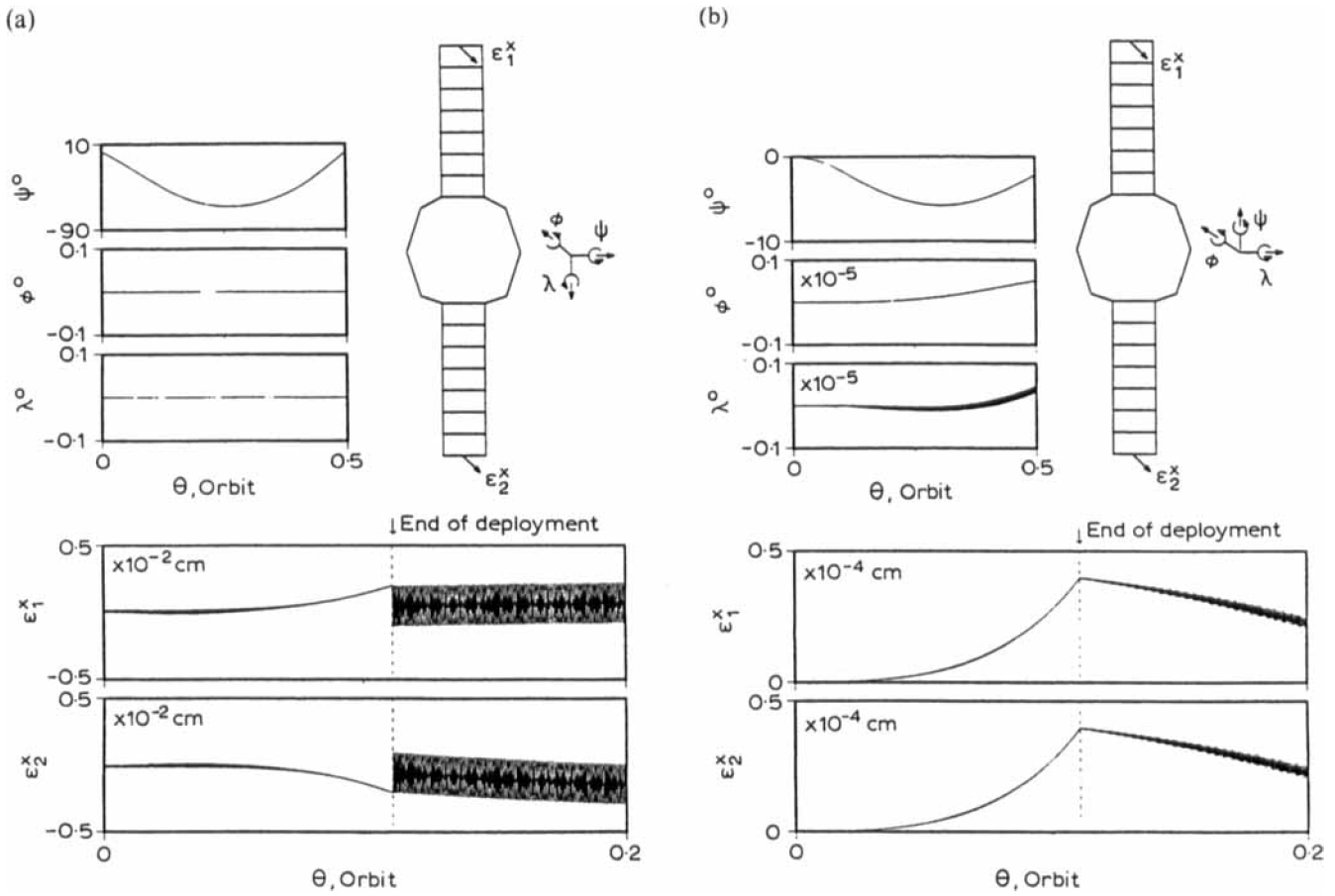

Fig. 11. Dynamical response of the SFU during deployment of the solar array pedals: (a) in-plane deployment. (b) Out-of-plane deployment.

The planned deployment/retrieval strategy of the SAPs can be separated into three stages as summarized below:

(i) The SAPs are deployed in 15 min with the longitudinal axis parallel to the local vertical, i.e. one SAP points towards the earth while the other away from the earth.
(ii) The SFU then undergoes a 90° roll so that the longitudinal axes of the SAPs are aligned with the orbit normal.
(iii) At the end of the mission, the SAPs are retrieved with the SFU in the same orientation as (ii). The retrieval time is also 15 min. Contingency plans are also drafted in the event that either SAP fails to deploy or retrieve. Since it is assumed that the pedal length varies from 3 to 9·7 m instead of from 0 to 9·7 m, the deployment/retrieval time is adjusted to 10 min. The deployment velocity is taken to be constant.

7.1 Dynamical response

Figure 11 shows the system response during the deployment of the SAP. With the panels deployed in the nominal orientation, the SFU response is shown in Fig. 11(a). Since the SAPs are deployed in the in-plane direction, only the pitch motion is excited. Although the SFU remains stable, it undergoes a large amplitude pitch motion reaching a minimum of −63°. As the SAP becomes more flexible during deployment, the tip deflection increases too; however, the SAPs hardly oscillate. As soon as the deployment terminates, the pedals start to vibrate with a peak-to-peak amplitude of about 0·0025 cm. Figure 11(b) studies the feasibility of an alternative deployment strategy. Here, the SFU undergoes a 90° roll before the deployment, i.e. the SAPs are deployed in the out-of-plane direction. Advantages of this strategy are obvious. The pitch libration has a considerably smaller amplitude with a minimum of −5·8°. At the end of deployment, the SAPs vibrate at amplitudes about two orders smaller than the corre-

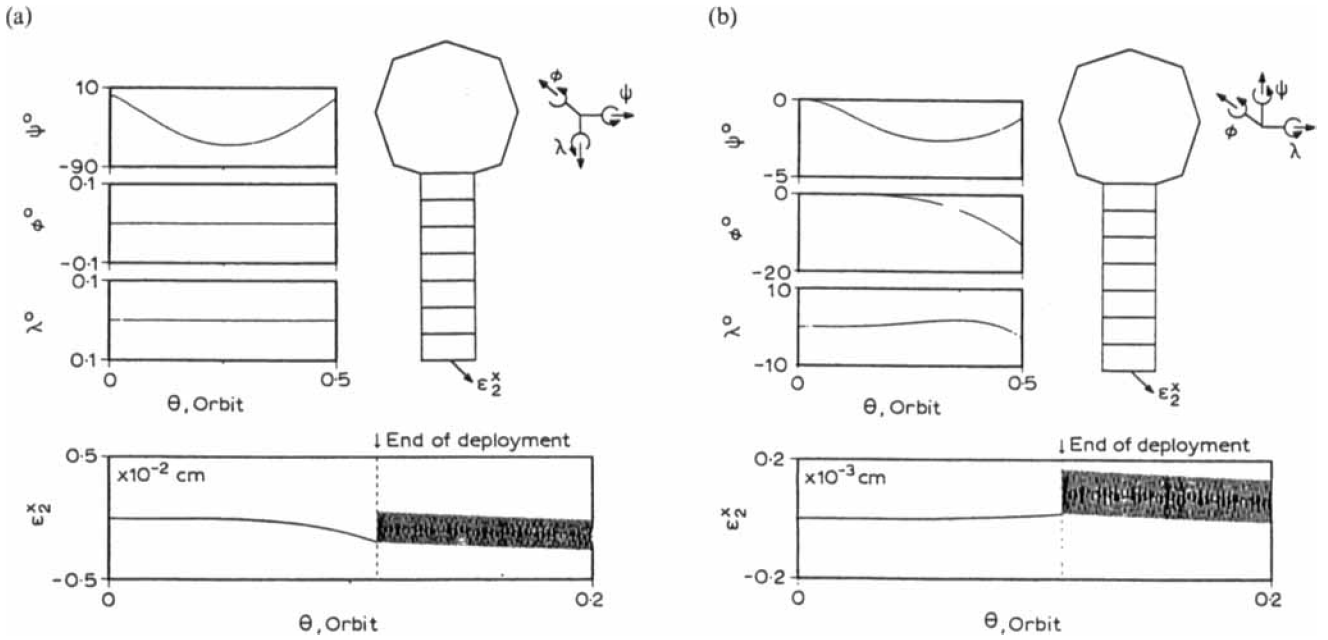

Fig. 12. Response characteristics of the SFU during deployment of one solar array pedal (B_2): (a) in-plane deployment. (b) Out-of-plane deployment.

sponding ones in Fig. 11(a). The only disadvantage with this strategy is that both roll and yaw are also excited; however, their amplitudes are of the order 10^{-5} even after 0·5 orbit.

Even if one SAP fails to deploy, the SFU remains stable under asymmetrical deployment (Fig. 12). Here, only B_2 is assumed to deploy successfully. In Fig. 12(a), B_2 is deployed in the direction towards the earth. The figure shows that both the libration and vibration responses remain essentially the same as if both the pedals were deployed. In contrast, when only B_2 is deployed in the out-of-plane direction, the SFU response is different from that in Fig. 12(b). Although the pitch motion has reduced its minimum amplitude to $-2{\cdot}6°$ from $-5{\cdot}8°$, the roll and yaw amplitudes increase significantly. With both the pedals deployed, the orders of magnitude of roll and yaw are about 10^{-5} at the end of 0·5 orbit. With only B_2 deployed, roll and yaw attain values of $-12{\cdot}9°$ and $-2{\cdot}7°$, respectively, over the same period. The SAP vibration trends also change. At the end of the deployment, the SAP oscillates with a peak-to-peak amplitude of 0·0002 cm. This value, though small, is about one order higher than that in the case with both SAPs deployed.

Figure 13 shows the system response during the SAP retrieval. The effect of retrieval time is studied here. In Fig. 13(a), a 5 min retrieval period is assumed. Even with this fast retrieval, the SFU remains stable with a maximum pitch angle of 6°, which is essentially of the same magnitude as that in the deployment case. The roll and yaw angles remain small but are considerably larger than those during the deployment. At the end of 0·5 orbit, their amplitudes are $-0{\cdot}0013°$ and $-0{\cdot}0005°$, respectively. As the SAPs become more rigid with the retrieval, it is reasonable that they attain a minimum deflection ($-0{\cdot}5 \times 10^{-5}$ cm) during retrieval and oscillate with a peak-to-peak amplitude of less than 10^{-7} cm afterwards. With the retrieval time increased to 10 min, the libration response remains unchanged (Fig. 13(b)). The SAP vibration retains the same response trend and about the same minimum deflection ($-0{\cdot}64 \times 10^{-5}$ cm).

Recall that the SFU remains stable for inplane or out-of-plane deployment of the SAPs. This is no longer true for the SAP retrieval. Although out-of-plane retrieval of the SAPs has no adverse effect on the SFU, in-plane retrieval tends to destabilize the system. With a 5 min in-plane retrieval, the SFU starts to tumble after 0·004 orbit (not shown). Over the same period, the tip deflections of the SAPs are over 50 cm. Even with the retrieval time increased to 10 min, the system remained unstable although the onset of tumbling motion was delayed to 0·008 orbit. When the retrieval time was further increased to 20 min, the system remained stable only up to 0·13 orbit. If either one of the SAPs fails to deploy or retrieve, the retrieval manoeuver turned out to be a critical situation. Whether the retrieval is performed out-of-plane or in-plane with B_1 or B_2, the system remains unstable (not shown).

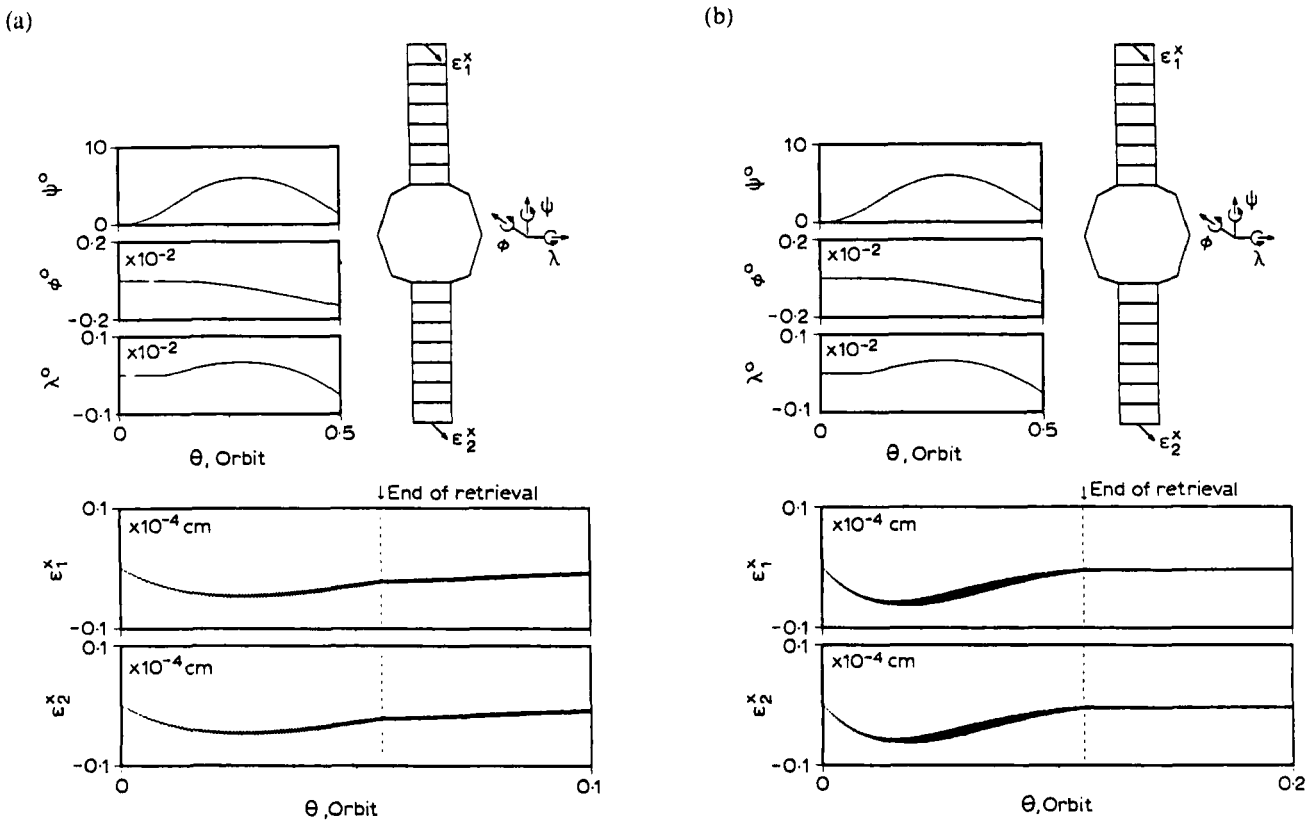

Fig. 13. Libration and vibration response of the SFU during out-of-plane retrieval of the solar array pedals: (a) 5 min retrieval period. (b) 10 min retrieval period.

8 CONCLUDING REMARKS

A rather general Lagrangian formulation for studying dynamics and control of a large class of spacecraft is introduced and its distinctive features summarized. The modal analysis carried out for two evolving configurations of the Space Station indicates the importance of the appendage flexibility. Also, the system modes are found to be strongly influenced by the main truss mass and module clusters. The application of the formulation is illustrated through numerical simulations of two spacecraft models. The PMC dynamical analysis points to the dominance of the power boom. A small power boom disturbance can induce large appendage displacement; however, a stinger disturbance has hardly any effect on the power boom. The desired velocity and microgravity level on the Space Station is found to be very stringent. Even a small initial displacement of the power boom or stinger results in velocity or acceleration level exceeding the design limit. The deployment of the SAPs of the SFU shows that the spacecraft remains stable under symmetric or asymmetric deployment. The parametric study also shows that the out-of-plane deployment has the advantage over the in-plane extension in terms of smaller pitch response. Retrieval of the SAP can lead to instability under certain critical situations. The out-of-plane symmetrical retrieval presents no problem. However, the unsymmetrical out-of-plane retrieval leads to instability even for a prolonged retrieval time. The SAP retrieval in the in-plane direction is found to be unstable. Regardless of the symmetry or period of retrieval, the spacecraft starts to tumble in a short period of time.

It would be appropriate to close with a few remarks concerning desirable directions for future efforts:

(i) The entire field is wide open to innovative contributions. Dynamics and control of such nonlinear, nonautonomous and coupled systems accounting for joint conditions, damping, external and internal nonconservative disturbances, etc., remain virtually untouched. Development of algorithms to predict the effect of mass, inertia, damping, environmental input, etc., on the dynamics and control parameters represents an exciting challenge.

(ii) With several relatively general formulations in hand and the programs operational, coordinated efforts should be made to develop a compre-

hensive data bank for multibody system dynamics and control. This should provide design charts over a wide range of system parameters and control strategies. Not only will it prove useful to design engineers involved in planning of future scientific, communications and other applied technology satellites but will also help in assessing dynamical, stability and control considerations associated with the time dependent evolving structures such as the Space Shuttle based construction of the proposed Space Station.

(iii) As a general approach to the problem gets well established, details should begin to receive more attention, e.g. quasi-steady, discrete or continuous representation of elastic appendages, modes to be used and their number from accuracy and computational considerations, robustness of control and step-size and numerical stability.

(iv) So far, the complex character of the problem has limited most analyses to small deformations, rigid body rotations and slewing manoeuvers. Studies aimed at dynamic response, stability and control in the large are, of course, formidable but promise to be equally exciting and rewarding.

(v) Finally, and perhaps most importantly, in order to validate and improve literally hundreds of algorithms aimed at flexible multibody dynamics and control, carefully planned ground and space based experiments are urgently needed.

ACKNOWLEDGEMENT

The investigation reported here was supported by the Natural Sciences and Engineering Research Council of Canada, Grant No. A-2181; and the Centers of Excellence Program, Grant No. IRIS/C-8, 5-55380.

REFERENCES

1. Berry, D. T., Yang, T. Y. & Skelton, R. E., Dynamics and control of lattice beams using simplified finite element models. *J. Guidance, Control, and Dynamics*, **8** (1985) 612–19.
2. Frisch, H. P., A digital computer program for the dynamic interaction simulation of controls and structures. In *Proc. Workshop on Multibody Simulation*, eds G. Man & R. Laskin, 1988, JPL D-5190, JPL Publisher, Pasadena, CA, USA, pp. 478–81.
3. Ho, J. Y. L., Direct path method for flexible multibody spacecraft dynamics. *J. Spacecraft and Rockets*, **14** (1977) 102–10.
4. Ho, J. Y. L., Herber, D. R., Clapp, B. R. & Schultz, R. J., ALLFLEX program—Simulation methodology. In *Proc. Workshop on Multibody Simulation*, eds G. Man & R. Laskin, 1988, JPL D-5190, JPL Publisher, Pasadena, CA, USA, pp. 811–56.
5. Hooker, W., Equations of motion for interconnected rigid and elastic bodies. *Celestial Mechanics*, **11** (1975) 337–59.
6. IMSL, *IMSL Library Reference Manual, Vol. 1.* IMSL Inc., Houston, TX, 1980, pp. DGEAR-1–9.
7. Ibrahim, A. M., Mathematical modelling of flexible multibody dynamics with application to orbiting systems. PhD dissertation, The University of British Columbia, Vancouver, Canada, 1988.
8. Juang, J. N. & Sun, C. T., System identification of large flexible structures by using simple continuum models. *The Journal of the Astronautical Sciences*, **31** (1983) 77–98.
9. Likins, P. W. & Bouvier, M. K., Attitude control of nonrigid spacecraft. *Astronautics and Aeronautics*, **9** (1971) 64–71.
10. Lips, K. W., *Dynamics of a large class of satellites with deploying flexible appendages.* PhD dissertation, The University of British Columbia, Vancouver, Canada, 1980.
11. Matsunaga, S., Miura, K. & Natori, M., A constructional concept for large space-based intelligent/adaptive structures. Paper presented at *31st AIAA/ASME/ASCE/AMS/ASC Structures, Structural Dynamics and Materials Conf.*, Long Beach, CA, April 1990, Paper No. 90–1128.
12. Meirovitch, L. & Quinn, R. D., Equations of motion for maneuvering flexible spacecraft. *J. Guidance, Control, and Dynamics*, **10** (1987) 453–65.
13. Misra, A. K. & Modi, V. J., The influence of satellite flexibility on orbital motion. *Celestial Mechanics*, **17** (1977) 145–65.
14. Misra, A. K. & Modi, V. J., 1983. Dynamics and control of tether connected two body systems—A brief review. In *Space 2000*. AIAA Publisher, New York, pp. 473–514.
15. Misra, A. K. & Modi, V. J., A survey on the dynamics and control of tethered satellite systems. In *Advances in the Astronautical Sciences*, ed. P. M. Bainum *et al.* American Astronautical Society, Washington, DC, USA, Vol. 62, 1986, pp. 667–719.
16. Miura, K. & Matsunaga, S. An attempt to introduce intelligence in space structures. Paper presented at *30th AIAA/ASME/ASCE/AHS/ASC Structures, Structural Dynamics and Materials Conf.*, Mobile, AL, April 1989, Paper No. 89–1289.
17. Modi, V. J., Attitude dynamics of satellites with flexible appendages—A brief review. *J. Spacecraft and Rockets*, **11** (1974) 743–51.
18. Modi, V. J. & Ibrahim, A. M., A general formulation for librational dynamics of spacecraft with deploying appendages, *J. Guidance, Control, and Dynamics*, **7** (1984) 563–9.
19. Modi, V. J. & Ng, A. C., Dynamics of interconnected flexible members in the presence of environmental forces: A formulation with applications. *Acta Astronautica*, **19** (1989) 561–71.
20. Modi, V. J. & Shrivastava, S. K., Satellite attitude dynamics and control in the presence of environmental torques—A brief review. *J. Guidance, Control, and Dynamics*, **6** (1983) 461–71.

21. Narayanaswami, R. & Adelman, H. M., Inclusion of transverse shear deformation in the finite element displacement formulations. *AIAA Journal*, **10** (1974) 1613–14.
22. NASA Space Station Program Office, *Space station engineering data book*. NASA Report No. SSE-E-87-R1, Washington, DC, 1987.
23. NASA Space Station Program Office, *Modal analysis of selected space station configurations*. NASA Report No. SSE-E-88-R8, Washington, DC, 1988.
24. Ng, A. C., Dynamics and control of orbiting flexible systems: A formulation with applications, PhD dissertation, The University of British Columbia, 1992.
25. Roberson, R. E., Two decades of spacecraft attitude control. *J. Guidance and Control*, **2** (1979) 3–8.
26. Sherman, M., SD/EXACT and SD/FAST—Symbolic manipulation codes. In *Proc. Workshop on Multibody Simulation*, eds G. Man & R. Laskin, 1988, JPL D-5190, JPL Publisher, Pasadena, CA, USA, pp. 692–726.
27. Singh, R. P., VanderVoort, R. J. & Likins, P. W., Dynamics of flexible bodies in tree topology—A computer-oriented approach, *J. Guidance, Control, and Dynamics*, **10** (1985) 584–90.
28. Small Space Platform Working Group, *Advanced Technology Experiment Onboard Space Flyer Unit (SFU)*. Institute of Space and Astronautical Science and Space Station Task Team, Sagamitava, Kanagawa, Japan, 1986, pp. 115–202.
29. Spanos, J. T. & Tsuha, W. S., Selection of component modes for the simulation of flexible multibody spacecraft. Paper presented at *AAS/AIAA Astrodynamics Specialist Conf.*, August 1989, Paper No. AAS-89–438.
30. Special Section, Large Space Structure Control: Early Experiments, *Journal of Guidance, Control, and Dynamics*, **7** (1984) 513–62.
31. Vu-Quoc, L., & Simo, J. C., Dynamics of Earth-Orbiting Flexible Satellites with multibody components, *J. Guidance, Control, and Dynamics*, **10** (1987) 549–58.
32. Wada, B. K., Adaptive Structures Pape presented at *30th AIAA/ASME/ASCE/AHS/ASC Structures, Structural Dynamics and Materials Conf.*, Mobile, AL, April 1989, Paper No. 89–1160.